Penerbit UTHM

© Universiti Tun Hussein Onn Malaysia Publisher's Office

JSMPM

http://publisher.uthm.edu.my/ojs/index.php/jsmpm

e-ISSN : 2821-2843

Journal of Sustainable Materials Processing and Management

Utilization of Oyster Shell Powder for Hydration and Mechanical Properties Improvement of Portland Cement Pastes

H. H. M. Darweesh[1*]

[1]Refractories, Ceramics and Building Materials Department,
National Research Centre, Dokki, Cairo, 12622, EGYPT

*Corresponding Author

DOI: https://doi.org/10.30880/jsmpm.2023.03.01.003
Received 18 January 2023; Accepted 20 March 2023; Available online 07 May 2023

Abstract: Supplementary cementitious materials (SCMs) are usually partially substituted at the expense of Portland cement (OPC) to reduce, as possible, the CO_2 emission. There has been limited studies involved the use of Oyster shell (OS) to replace OPC. The current study investigated the properties of a ternary base batch containing Oyster shell powder (OSP). The ternary cement batch was consisting of OPC, granulated blast furnace slag (GbfS) and metakaolin (MK). The results indicated that the water consistency and setting times (initial and final) are gradually increased. The water absorption and total porosity are decreased, while the bulk density and combined water content increased. This behaviour continued up till 16 % OSP content, but then reverse was obtained with any further increase of OSP content. The same trend was achieved with the compressive strength. The addition of OSP often formed mono- and/or hemicarbonate instead of monosulfate because it is mainly composed of carbonates, and moreover it is stabilizing the formation of trisulphate or ettringite in the hydrated samples. The decrease is not the decrease of free lime contents proved that the OSP is a pozzolanic material. This was confirmed by FT-IR spectra. From the results it could be concluded that the optimum content of OSP was at most 16 %.

Keywords: Cement, slag, metakaolin, oyster shell, density, porosity, strength

1. Introduction

Production of Ordinary Portland cement (OPC) produces a large amount of CO_2 (5–8 %) of its global emissions [1,2]. So, the strategies of OPC production are now used to reduce the CO_2 emission footprint of concrete by replacing OPC with supplementary cementitious materials (SCMs) [3-6]. Calcium sulfoaluminate (CSA) cement [7,8] is an alternative cementitious binder to OPC and it has been intensively investigated because of its low CO_2 emissions during its production and excellent setting and mechanical properties. It was reported that 6 % limestone (LS) in CSA cement is so effective that it accelerated the hydration of this cement and moreover it decreased the total porosity of the hardened samples. This is due to that LS in CSA cement forms hemicarbonate and monocarbonate that could be stabilized the ettringite phase leading to the increment of mechanical properties [9-11]. Using of fly ash (FA) in CSA cement is an effective strategy to lower both cost and CO_2 emissions [12–15]. The addition of 5–15 wt % FA to CSA cement increased the compressive strength by 3–6 MPa after 28 days of hydration. The higher amounts of FA were adversely reflected on the mechanical strength [12–14]. The use of 5-30 wt % granulated blast furnace slag (GBFS) does not lower the compressive strength [2,16]. The SCMs incorporated in CSA cements without lowering in the mechanical properties is slightly lower than those in OPC. This is attributed to that the pH in the pore solutions of CSA cements is nearly lower than that of OPC, and portlandite. The later phase may be reacted with SCMs in hydrated CSA cements, but in a lower degree of reaction of SCMs in hydrated CSA cements than in hydrated OPC [8,17,18]. The use

*Corresponding author: hassandarweesh2000@yahoo.com

of GbfS is most suitable for the high late strength development, while the use of LS and FA have a slight effect to improve the mechanical strength [19].

Though the significance to lower CO_2 footprint or to promot the comparable mechanical and durability performance are good, unfortunately investigation of PC-CSA-SCM ternary cements is too limited [20–23]. The present research attempted to address that by using various compositions with a constant increment. Ternary cement provides the opportunity to utilize the individual benefits of the binders simultaneously [24,25], where the replacement of cement with CSA in the ternary system ensures the reduction of CO_2 emission as CSA production requires a lower lime content [26–28]. Improving the mechanical and durability properties of the cement mixes is another benefit that can be obtained while using CSA [4,29-33].

Oysters generated a significant quantity of waste as oyster shells, which is mainly composed of calcium carbonates ($CaCO_3$) [34-36]. The benefits of adding $CaCO_3$ to OPC cement was reported showing the improvement of early strength, porosity and other durability properties [36]. However, most of this research concentrated on LS as a source of $CaCO_3$ [36-38]. Recently, the use of OST powder as an essential source of $CaCO_3$ is becoming a research focus as it is readily available in the form of waste. Addition of a higher amount of oyster's shells have a negative impact on the strength and workability of cement mixes. However, the addition percentage of OST addition (15-35 %) where the negative impact becomes severe enough to compromise the mechanical and durability characteristics of the system [34,39,40].

The study investigated the effect of the addition of oyster shell powder (OSP) on the properties of OPC-GbfS-MK ternary cement, where GbfS and metakaolin (MK) were used as SCMs. MK has been found to improve the physical and mechanical properties [18,35,41,42]. The OSP was added to Portland cement (OPC)-GbfS (GbfS)-MK (MK) to investigate its effect on reaction pathways and cement properties with the aim to optimize the amount of OSP to be added to cement.

2. Experimental

2.1 Raw Materials

The raw materials that were used in the current study are ordinary Portland cement (OPC), granulated blast furnace slag (GbfS), metakaolin (MK), and Oyster shell (OS). The OPC sample (OPC Type I- CEM I 42.5 R) was delivered from Sakkara cement factory, Giza, Egypt, and its commercial name is known as "Asmant El-Momtaz". The GbfS sample was supplied by Iron and Steel Company, Helwan, Egypt. The MK sample is one of these calcined clays, where it arises from the calcination of kaolinitec clays [41]. The MK sample was as a pozzolanic material to improve most of the cement properties. The oyster shell sample was delivered from a local marine plant. The oyster shell sample was first washed with water to remove any organic impurities, and then let too dry before being crushed and grounded to pass through 325-mesh sieve to a very fine powder (OSP). The surface areas of the raw materials were 3450, 4560, 4045, 5365 cm^2/g, respectively. The surface area of the raw materials was carrried out using Air-permeabilty Apparatus. The chemical composition that was carried by X-ray fluorescence (XRF) and the particle size distribution analysis that was conducted with sieving of the used raw materials are shown in Table 1 and Table 2, respectively. The mixture proportions used are listed in Table 3.

Table 1 - Chemical composition of the used raw materials, wt.%

Oxide	OPC	GbfS	MK	OSP
SiO_2	19.36	31.45	49.48	1.39
Al_2O_3	4.31	14,03	47.37	1.25
Fe_2O_3	3.54	0.43	1.26	1.11
CaO	61.87	46.16	0.29	57.03
MgO	1.39	3.24	-----	0.27
MnO	-----	0.41	-----	-----
Na_2O	1.31	0.31	-----	0.63
K_2O	1.07	0.59	0.22	0.07
TiO_2	0.29	0.84	2.23	-----
P_2O_5	0.13	-----	0.11	0.08
SrO	0.08	-----	-----	0.13
Cl^-	-----	-----	-----	0.24
SO_3	2.12	1.73	-----	0.69
LOI	4.53	0.81	0.84	37.11
Total	100	100	100	100

Table 2 - Particle size distribution of the used raw materials, µm

Materials	Particle size distribution, µm					
Size	> 63	63-16	16-8	8-2	< 2	Total
B	1.21	1.34	2.43	6.15	88.87	100
OSP	0.14	0.13	0.68	2.84	96.21	100

Table 3 - Mix constitutions from the used raw materials, wt. %

Batch	Base batch	OSP
S0	100	-----
S1	96	4
S2	92	8
S3	88	12
S4	84	16
S5	80	20

According to the mix design, the dry mixtures were mixed for 1 min using a mechanical mixer. Subsequently, water was added and mixed for 3 min. Fresh paste samples were transferred to a mold and sealed with a plastic wrap. The samples were cured under sealed conditions at a temperature of 20–23 °C till the designated time of testing (1, 3, 7, 28 and 90 days).

2.2 Preparation and Methods

The base cement batches were composed from OPC, GbfS and MK with ratios as 90:5:5, respectively. The OSP was partially substituted at the expence of the base batch with the ratios of 4, 8, 12, 16 and 20. Having the symbols: S0, S1, S2, S3, S4 and S5, respectively. The blending process of the various cement mixes was carried out in a porcelain ball mill using three balls for two hours to assure the complete homogeneity of all cement mixes. During casting, 1 % polycarboxylic ether as a high reducing water superplasticizer admixture was added to the mixing water which in turn added to the prepared cement mixes to avoid the agglomeration of the nanoparticles of the used raw materials and to improve cement dispersion as well as to arrest further hydration.

The standard water consistency (WC) as well as setting time (initial and final) of the various cement pastes were directly determined using Vicat Apparatus [42-45]. The cement pastes were then cast using the predetermined water of consistency, moulded into one-inch cubic stainless steel moulds (2.5 x 2.5 x 2.5 cm^3) using about 500 g cement mix, vibrated manually for three minutes and then on a mechanical vibrator for another three minutes. The surface of the moulds was smoothed using a suitable spatula. Thereafter, the moulds were kept in a humidity chamber for 24 hours under 95 ± 1 RH and room temperature, demoulded in the next day and soon immersed in water till the time of testing at 1, 3, 7, 28 and 90 days. The bulk density (BD), total porosity (δ) and the compressive strength (CS) of the various hardened cement pastes [42-45] were measured.

Thereafter, about 10 grams of the broken specimens were first well ground, dried at 105°C for an hour, and then were placed in a solution mixture of 1:1 methanol: acetone to stop the hydration [46,47]. About 10 grams of the broken specimens from the determination of compressive strength were first well ground, dried at 105°C for 30 min., and then were placed in a solution mixture of 1:1 methanol: acetone to stop the hydration [46,47]. The chemically-bound water content was measured, where bout one gram of the sample was first dried at 105°C for 24h, and then the chemically-bound water content (BWn) at each hydration age was determined on the basis of ignition loss at 1000°C for 30 min. soaking [42-44,48].

The pozzolanic activity was detected by measuring the free lime content (FLn) of the hydrated samples pre-dried at 105°C for 24h. About 0.5 g of the sample + 40 ml ethylene glycol → heating to about 20 minutes without boiling. About 1–2 drops of pH indicator were added to the filtrate and then titrated against freshly prepared 0.1N HCl until the pink colour disappeared. The 0.1N HCl was prepared using the following equation: Where, Wn, W1 and W2 are combined water content, weight of sample before and after ignition, respectively. The free lime content of the hydrated samples pre-dried at 105°C for 24h was also determined. About 0.5g sample +40 ml ethylene glycol → heating to about 20 minutes without boiling. About 1–2 drops of pH indicator were added to the filtrate and then titrated against freshly prepared 0.1N HCl until the pink colour disappeared. The heating and titration were repeated several times until the pink colour did not appear on heating [46,47,49].

The DTA-TGA analysis was carried out using NETZSCH Geratobau Selb, Bestell-Nr. 348472c at a heating rate 10 °C/min up to 1000 °C. The electrical conductivity test [50,51] consisted of measuring the electrical conductivity at pre-set times in a solution with 0.45 g of calcium hydroxide, 250 ml of deionized water and 5.25 g of the BLA. The relative difference in conductivity for a given time is determined as a function of the initial conductivity. Based on the electrical

conductivity values proposed by Lux´an [50] the materials are classified according to their pozzolanicity. The obtained results are confirmed with fourier transform infared spectra (FT-IR) and scanning electron microscopic (SEM) analysis. The FT-IR was performed by Pye-Unicum SP-1100 in the range of 4000-400 cm^{-1} and a resolution of 500 cm^{-1}. The FT-IR analysis was done in the National Research Centre, Dokki, Cairo, Egypt. The SEM microscopy was conducted for some selected samples by using JEOL–JXA–840 electron analyzer at accelerating voltage of 30 KV. The fractured surfaces were fixed on Cu-kα stubs by carbon paste and then coated with a thin layer of gold.

3. Results and Discussion

3.1 Construction of References

(a) Water of Consistency and Setting Time

Fig. 1 shows the water of consistency and setting times (initial and final) of the various cement pastes that composed of the base batch (S0) which was substituted with the various ratios of OSP waste (S1-S5). It is obvious that the water of consistency increased as the OSP content increased. This is mainly contributed to the fact that the OSP is very voracious to water so that it needs a large amount of water to form standard cement pastes [48-51]. The same trend was displayed by the setting time. Therefore, the B5 recorded the highest amount of water consistency and the longest times of setting, whereas S0 achieved the lowest. The measured water of consistency was used in all of the foreward tests.

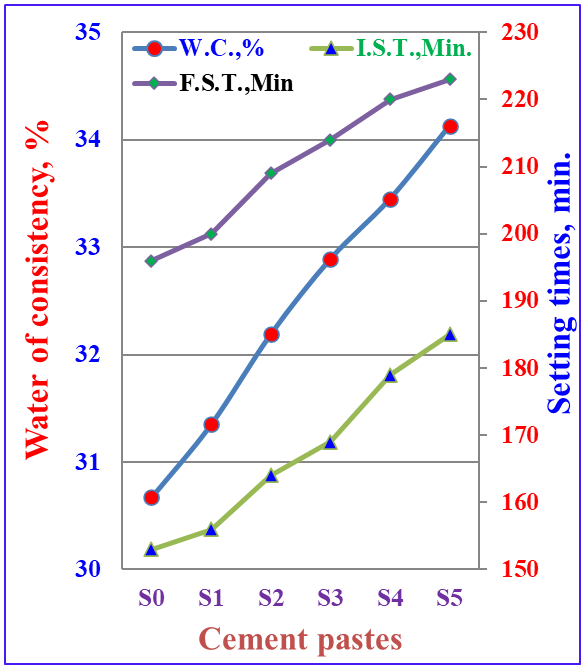

Fig. 1 - Water of consistency and setting time of the various cement pastes with and without OSP waste

(b) Water Absorption

The water absorption (WA) of the various hardened cement pastes (S0-S5) at 1, 3, 7, 28 and 90 days are shown in Fig. 2. Generally, the WA of the reference base batch sample (S0) was decreased with the addition of OSP waste only up to 16 wt. % (S4), and then slightly increased with the further increase of OSP content (S5). The decrease of WA is mainly contributed to the higher compaction effect by higher surface area or fineness of the OSP particles which reflected positively on the results of WA, where it reduced the pore volume of the hardened cement pastes [52,53]. The increase of WA is essentially attributed to the large deficiency of the main binding material [54,55]. Consequently, the greater amount of this waste must be avoided.

(c) Total Porosity

The total porosity of the different hardened cement pastes containing various ratios of OSP (S0-S5) was represented as a function of curing time up to 90 days in Fig. 3. The total porosity of the reference (S0) at any curing time was decreased with the increase of OSP content, but only up to 16 % (S4), and then reincreased with any further increase of OSP (S5). The decrease of total porosity is primirily attributed to the hydration of the main phases of the cement, and moreover it is due to the pozzolanic activity of GbfS and MK [55-58]. In addition to the pozzolanic

reactivity of OSP with the resulting Ca $(OH)_2$ coming from the normal hydration process of the silicate phases of the cement (C_3S and β–C_2S) forming additional CSHs that precipitated into the pore structure. This reduced the total porosity [48,52,53]. The reincreased values of the total porosity with higher content of OSP than 16 % (S5) is mainly attributed to the larger deficiency of the main binding material (S0) which is responsible for the hydration process [48,49,59]. So, the higher amounts of OSP than 16 % is undesired.

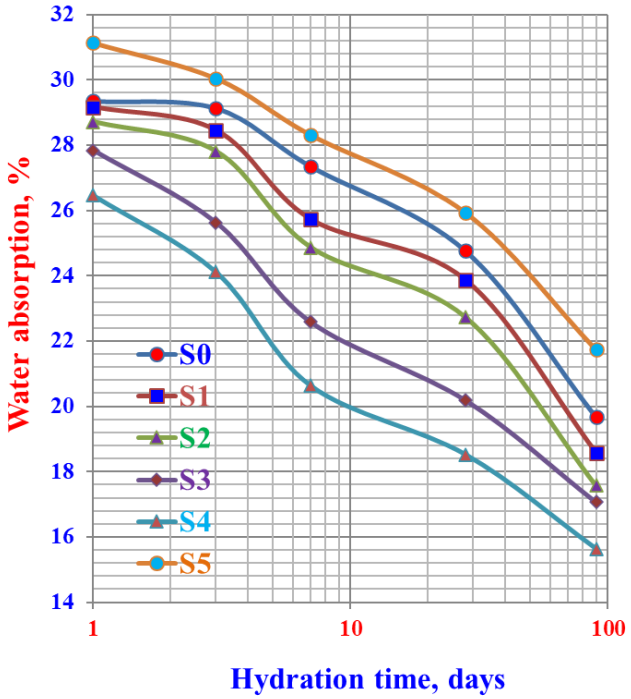

Fig. 2 - Water absorption of the various cement pastes with and without OSP hydrated up to 90 days

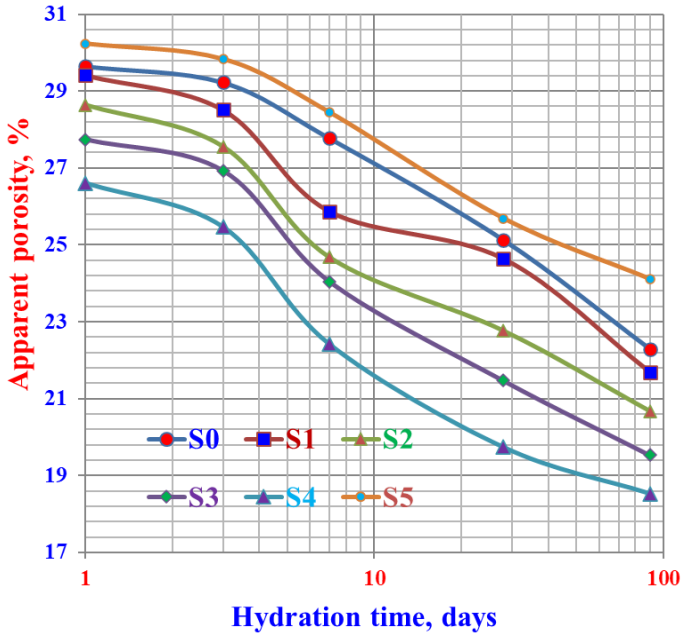

Fig. 3 - Apparent porosity of the various cement pastes with and without OSP hydrated up to 90 days

(d) Bulk Density

The results of bulk density of the various hardened cement pastes containing different ratios of OSP (S0-S5) hydrated up to 90 days are presented in Fig. 4. Generally, the bulk density slightly increased with the incorporation of OSP up till 16 % (S4), and then decreased by the further increase of OSP (S5). The increase of bulk density is mainly due to the deposition of the formed CSHs that resulting from the hydration of the main phases of the cement and also

the additional CSHs that resulted from the pozzolanic reactions of GbfS, MK and OSP particles with the free lime, Ca $(OH)_2$ coming from the hydration of the calcium silicate phases of the cement, C_3S and β–C_2S [52,53,59], while the slight reduction in the bulk density is contributed to the lower specific gravity of the OSP compared to that of OPC, GbfS and MK [48,54,59]. Also, the hardened cement pastes with OSP showed a lower water absorption and a lower porosity especially at 90 days. The better performance of the cement pastes with OSP is due to the combined effect of pozzolanic activity and the filler effect of nanosized particles of three waste materials (GbfS, MK and OSP), resulting in the refinement of the pores of the cement pastes. Therefore, the reduction of water absorption and total porosity were resulted [49,51,53,54,59,60]. It is good mention that the rate of the normal hydration of the base batch (S0) is often decreased due to the addition of OSP. So, the formed amount of CSHs was reduced with higher addition of OSP, this was compensated by the pozzolanic reactions of GbfS, MK and OSP with the free lime, Ca $(OH)_2$ resulting from the hydration of calcium silicate phases of the cement. As a result, the higher quantities of OSP must be avoided.

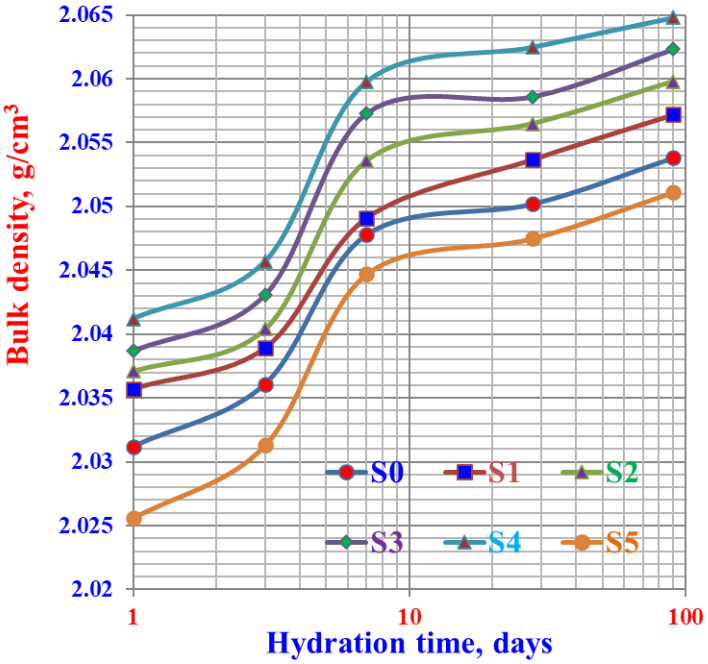

Fig. 4 - Bulk density of the various cement pastes with and without OSP hydrated up to 90 days

Table 1 - An example of a table

An example of a column heading	Column A (*t*)	Column B (*t*)
And an entry	1	2
And another entry	3	4
And another entry	5	6

3.2 Chemical Properties

(a) Chemically-Bound Water Content

Fig. 5 illustrates the results of chemically-bound water contents of the various cement pastes containing different ratios of OSP (S0-S5) are drawn as a function of the hydration time up to 90 days. The bound water content of the blank (S0) was improved and enhanced as the hydration time progressed up to 90 days. This is principally attributed to the normal hydration process of the major phases of the cement [41,42]. With the addition of OSP, the bound water content was further improved and increased till 16 % from OSP content (S4), and then was suddenly decreased (S5). The increase of bound water content was firstly contributed to the usual hydration process of the major cement phases, in addition to the pozzolanic reaction effect of the three pozzolanic waste materials (GbfS, MK and OSP), whereas the decrease of bound water content is distinctly due to the large deficiency of the main binding material of the cement [44-54]. As a result, the optimum OSP content is only 16 % (S4). Hence, the higher OSP content is undesirable due to its adverse effect.

(b) Free Lime Content

The free lime contents of the different cement pastes containing OSP (S0-S5) hydrated up to 90 days are graphically represented as a function of hydration time in Fig. 6. The free lime content of the control (S0) was gradually increased with the hydration time up to 90 days. This is mainly attributed to the normal hydration of the di- and tricalcium silicates of the cement (C_2S and β-C_3S) to form CSHs [41,42]. With the incorporation of OSP at the expense of the base batch of the cement, the free lime content slightly decreased with the time of hydration till 90 days. This is essentially contributed to the pozzolanic reactivity of the GbfS, MK and also OSP with the resulting free lime, Ca $(OH)_2$ forming additional CSHs [38,52,54]. The decrease of the main cement phases responsible for yielding the free lime is another factor to decrease the free lime content.

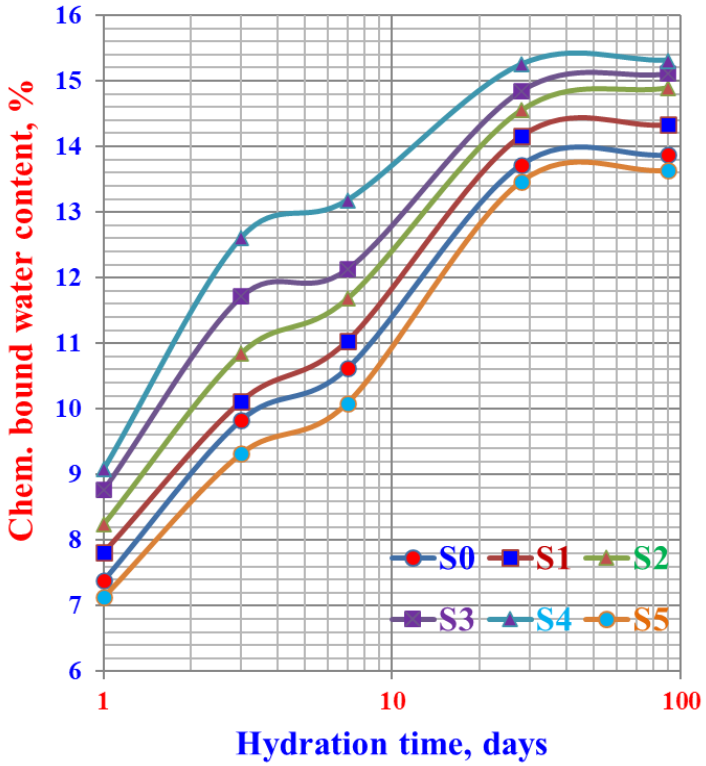

Fig. 5 - Chemically-bound water content of the various cement pastes with and without OSP hydrated up to 90 days

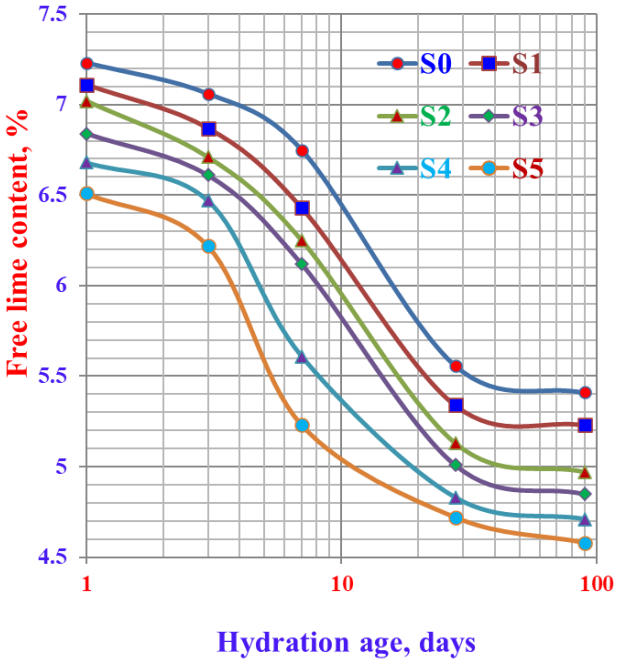

Fig. 6 - Free lime contents of the various cement pastes with and without OSP hydrated up to 90 days

3.3 Compressive Strength

The compressive strength of the various cement mixes containing OSP waste (S0-S5) hydrated up to 90 days are indicated in Fig. 7. The compressive strength of the hardened cement pastes improved and enhanced as the hydration time proceeded up to 90 days. This is mainly due to the normal hydration process of the major phases of the cement [38,41,42,53]. The compressive strength was further increased as the OSP content increased, but only up to 16 % (S4), and then decreased with any further increase of OSP content (S5). Furthermore, the increase of the compressive strength is also attributed to the filling performance and pozzolanic reactivity of GbfS, MK and OSP materials [44,51-54], while the decrease of compressive strength may be contributed to the detrimental characteristics of the very high specific surface area of OSP waste that created the agglomeration of the cement particles. This worse performance effect is associated with the lower cement content that influences the direct reduction of the primary hydration products responsible to improve the compressive strength (CSH) and its negatively reflection on the rate of Ca^{2+} release that delaying the precipitation of calcium hydroxide [55]. Therefore, it reduces its availability for the development of pozzolanic reactions with the OSP waste particles. Thus, the ideal limit of OSP to be incorporated in the cement (S0) is only 16 % (S4) at the most, because with the higher percentages (S5), the filler effect of the particles and the availability of Ca $(OH)_2$ in the hydration reaction are reduced [56,57]. On the other hand, the large deficiency of the main binding material of the cement is the main cause of decreasing the compressive strength. The low crystallinity of OSP waste prefers the developing of pozzolanic reactions, allowing secondary CSHs formation to takes place. As a result, the combination of these effects, the porous structure of the hardened cement pastes is refined [57-64]. It could be concluded that the rate of the normal hydration process of the control (S0) is often declined due to the replacement of OSP waste at the expense of the base batch (S0). So, the quantity of the formed CSHs was diminished. This was compensated by the pozzolanic reactions of GbfS, MK and OSP with the free lime, Ca $(OH)_2$ coming from the hydration of di- and tricalcium silicate phases of the cement.

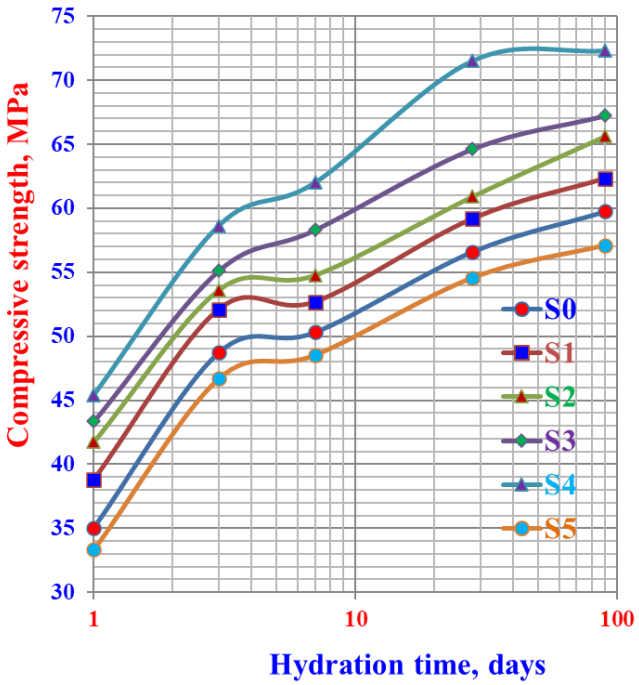

Fig. 7 - Compressive strength of the various cement pastes with and without OSP hydrated up to 90 days

3.4 FT-IR Spectra

Fig. 8 indicates the FT-IR spectra of the cement batches S0, S3 and S4 cured up to 90. The sharp absorption band at wave number 3637-3643 cm^{-1} is due to the free OH^{-1} coordinated to Ca^{2+}, i.e., free lime, $Ca(OH)_2$, which was abbreviated as CH. The intensity of the free lime absorption band of the control (S0) is slightly obvious due to the presence of two pozzolanic materials (GbfS and MK) that were reacted with the released CH to form CSH. It was completely disappeared with S3 and S4 due to the incorporation of SOP ash. This is mainly attributed to its active pozzolanic effect that initiated and improved the rate of hydration [35,42,43,54,60-64]. The broad absorption band intensity at wave number 3793-3025 cm^{-1} which is due to the OH^{-1} group associated to H^+ bond (H_2O) increased with the incorporation of OSP ash due to the absorption of large quantity of water to form CSH. The intensity of the absorption band of CSH was improved with OSP ash. The two absorption bands nearly at 1723-1638 and 1569-1153 cm^{-1} are contributed to the main silicate band involve Si-O stretching vibration bands of CSH. The formed CSHs in S4 was higher than that of others. The three absorption bands at 1117-687 cm^{-1} which characterizing CO_3^{2-} and SO_4^{2-}, respectively, enhanced with OSP ash content. This is certainly due to the rate of carbonation and sulfonation of CSH and /or CSAH.

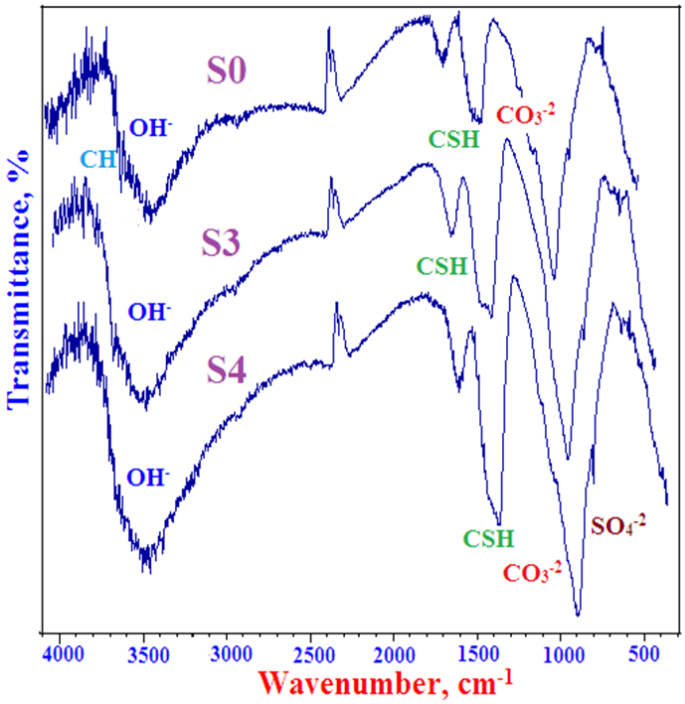

Fig. 8 - FT-IR spectra of the cement pastes S0, S3 and S4 hydrated at 90 days

4. Conclusion

The influence of OSP addition on the physical, chemical, and mechanical properties of OPC-GbfS-MK cement system was investigated. The addition of OSP, which mainly composed of calcium carbonate, allows the formation of mono- and/or hemicarbonates instead of monosulfate. This is in turn stabilizes the formation of trisulphate or ettringite. The incorporation of OSP reduces the amount of free lime or portlandite. The increase of the chemically-bound water content in the cement system was accompanied with an increase in the total amount of the CSHs. The presence of GbfS enhanced the OSP uptake, which results in the formation of more ettringite. Therefore, S4 mix containing 16 % was selected to be the better OSP uptake while maximizing the benefits obtained from each binder. Therefore, the optimum OSP content is 16 %.

Acknowledgement

The author gratefully acknowledged the support of the National Research Centre.

References

[1] Kajaste, R., & Hurme, M. (2016). Cement industry greenhouse gas emissions–management options and abatement cost. *Journal of Cleaner Production*, *112*, 4041-4052.

[2] Seo, J., Kim, S., Park, S., Yoon, H. N., & Lee, H. K. (2021). Carbonation of calcium sulfoaluminate cement blended with blast furnace slag. *Cement and Concrete Composites*, *118*, 103918.

[3] Miller, S. A., & Myers, R. J. (2019). Environmental impacts of alternative cement binders. *Environmental Science & Technology*, *54*(2), 677-686.

[4] Juenger, M. C., & Siddique, R. (2015). Recent advances in understanding the role of supplementary cementitious materials in concrete. *Cement and Concrete Research*, *78*, 71-80.

[5] Lothenbach, B., Scrivener, K., & Hooton, R. D. (2011). Supplementary cementitious materials. *Cement and Concrete Research*, *41*(12), 1244-1256.

[6] Lothenbach, B., Le Saout, G., Gallucci, E., & Scrivener, K. (2008). Influence of limestone on the hydration of Portland cements. *Cement and Concrete Research*, *38*(6), 848-860.

[7] Scrivener, K., Martirena, F., Bishnoi, S., & Maity, S. (2018). Calcined clay limestone cements (LC3). *Cement and Concrete Research*, *114*, 49-56.

[8] Martin, L. H., Winnefeld, F., Tschopp, E., Müller, C. J., & Lothenbach, B. (2017). Influence of fly ash on the hydration of calcium sulfoaluminate cement. *Cement and Concrete Research*, *95*, 152-163.

[9] Jeong, Y., Hargis, C. W., Chun, S., & Moon, J. (2017). Effect of calcium carbonate fineness on calcium sulfoaluminate-belite cement. *Materials*, *10*(8), 900.

[10] Pelletier-Chaignat, L., Winnefeld, F., Lothenbach, B., & Müller, C. J. (2012). Beneficial use of limestone filler with calcium sulphoaluminate cement. *Construction and Building Materials*, *26*(1), 619-627.
[11] Martin, L. H., Winnefeld, F., Müller, C. J., & Lothenbach, B. (2015). Contribution of limestone to the hydration of calcium sulfoaluminate cement. *Cement and Concrete Composites*, *62*, 204-211.
[12] García-Maté, M., De la Torre, A. G., León-Reina, L., Aranda, M. A. G., & Santacruz, I. (2013). Hydration studies of calcium sulfoaluminate cements blended with fly ash. *Cement and Concrete Research*, *54*, 12-20.
[13] Darweesh, H. H. M. (2021) Nano-glass waste substitution for portland cement pastes, *NanoProgress*, 3(6), 51-59.
[14] Ioannou, S., Reig, L., Paine, K., & Quillin, K. (2014). Properties of a ternary calcium sulfoaluminate–calcium sulfate–fly ash cement. *Cement and Concrete Research*, *56*, 75-83.
[15] Ma, B., Li, X., Shen, X., Mao, Y., & Huang, H. (2014). Enhancing the addition of fly ash from thermal power plants in activated high belite sulfoaluminate cement. *Construction and Building Materials*, *52*, 261-266.
[16] Yoon, H. N., Seo, J., Kim, S., Lee, H. K., & Park, S. (2021). Hydration of calcium sulfoaluminate cement blended with blast-furnace slag. *Construction and Building Materials*, *268*, 121214.
[17] Winnefeld, F., & Lothenbach, B. (2010). Hydration of calcium sulfoaluminate cements—Experimental findings and thermodynamic modelling. *Cement and Concrete Research*, *40*(8), 1239-1247.
[18] Darweesh, H. H. M. (2020) Metakaolin blended cement pastes, *International Journal of Innovative Studies in Sciences and Engineering Technology*, 6(1), 5-18.
[19] Gastaldi, D., Bertola, F., Irico, S., Paul, G., & Canonico, F. (2021). Hydration behavior of cements with reduced clinker factor in mixture with sulfoaluminate binder. *Cement and Concrete Research*, *139*, 106261.
[20] Afroughsabet, V., Biolzi, L., Monteiro, P. J., & Gastaldi, M. M. (2021). Investigation of the mechanical and durability properties of sustainable high performance concrete based on calcium sulfoaluminate cement. *Journal of Building Engineering*, *43*, 102656.
[21] Huang, T., Li, B., Yuan, Q., Shi, Z., Xie, Y., & Shi, C. (2019). Rheological behavior of Portland clinker-calcium sulphoaluminate clinker-anhydrite ternary blend. *Cement and Concrete Composites*, *104*, 103403.
[22] Zhang, J., Li, G., Yang, X., Ren, S., & Song, Z. (2018). Study on a high strength ternary blend containing calcium sulfoaluminate cement/calcium aluminate cement/ordinary Portland cement. *Construction and Building Materials*, *191*, 544-553.
[23] Pelletier, L., Winnefeld, F., & Lothenbach, B. (2010). The ternary system Portland cement–calcium sulphoaluminate clinker–anhydrite: hydration mechanism and mortar properties. *Cement and Concrete Composites*, *32*(7), 497-507.
[24] Vance, K., Aguayo, M., Oey, T., Sant, G., & Neithalath, N. (2013). Hydration and strength development in ternary portland cement blends containing limestone and fly ash or metakaolin. *Cement and Concrete Composites*, *39*, 93-103.
[25] Darweesh, H. H. M. (2022) Water permeability, strength development and microstructure of activated pulverized rice husk ash geopolymer cement, *NanoNEXT*, 3(1), 5-22.
[26] Li, P., Gao, X., Wang, K., Tam, V. W., & Li, W. (2020). Hydration mechanism and early frost resistance of calcium sulfoaluminate cement concrete. *Construction and Building Materials*, *239*, 117862.
[27] García-Maté, M., Santacruz, I., Ángeles, G., León-Reina, L., & Aranda, M. A. (2012). Rheological and hydration characterization of calcium sulfoaluminate cement pastes. *Cement and Concrete Composites*, *34*(5), 684-691.
[28] Hanein, T., Galvez-Martos, J. L., & Bannerman, M. N. (2018). Carbon footprint of calcium sulfoaluminate clinker production. *Journal of Cleaner Production*, *172*, 2278-2287.
[29] Bernardo, G., Telesca, A., & Valenti, G. L. (2006). A porosimetric study of calcium sulfoaluminate cement pastes cured at early ages. *Cement and Concrete Research*, *36*(6), 1042-1047.
[30] Darweesh, H. H. M. (2021) Low heat blended cements containing nanosized particles of natural pumice alone or in combination with granulated blast furnace slag, *NanoProgress*, 3(5), 38-46.
[31] Darweesh, H. H. M. (2021) Physical and chemo/mechanical behaviors of fly ash and silica fume belite cement pastes- Part I, *NanoNext*, 2(2), 1-15.
[32] Özbay, E., Erdemir, M., & Durmuş, H. İ. (2016). Utilization and efficiency of ground granulated blast furnace slag on concrete properties–A review. *Construction and Building Materials*, *105*, 423-434.
[33] Yang, K. H., Jung, Y. B., Cho, M. S., & Tae, S. H. (2015). Effect of supplementary cementitious materials on reduction of CO2 emissions from concrete. *Journal of Cleaner Production*, *103*, 774-783.
[34] Han, Y., Lin, R., & Wang, X. Y. (2022). Performance of sustainable concrete made from waste oyster shell powder and blast furnace slag. *Journal of Building Engineering*, *47*, 103918.
[35] Darweesh, H. H. M. (2022). Geopolymer cement based on bioactive eggshell waste or commercial calcium carbonates. *Research & Development in Material Science*, *17*(1), 1907-1916.
[36] Darweesh, H. H. M., & MR, A. E. S. (2019). Influence of sugarcane bagasse ash substitution on Portland cement characteristics. *Indian Journal of Engineering*, *16*, 252-266.
[37] Wang, X. Y. (2018). Analysis of hydration and strength optimization of cement-fly ash-limestone ternary blended concrete. *Construction and Building Materials*, *166*, 130-140.

[38] Adu-Amankwah, S., Zajac, M., Stabler, C., Lothenbach, B., & Black, L. (2017). Influence of limestone on the hydration of ternary slag cements. *Cement and Concrete Research*, *100*, 96-109.
[39] Attah, I. C., Etim, R. K., & Sani, J. E. (2019). Response of oyster shell ash blended cement concrete in sulphuric acid environment. *Civil and Environmental Research*, *11*(4), 62-74.
[40] Boháč, M., Palou, M., Novotný, R., Másilko, J., Všianský, D., & Staněk, T. (2014). Investigation on early hydration of ternary Portland cement-blast-furnace slag–metakaolin blends. *Construction and Building Materials*, *64*, 333-341.
[41] Medjigbodo, G., Rozière, E., Charrier, K., Izoret, L., & Loukili, A. (2018). Hydration, shrinkage, and durability of ternary binders containing Portland cement, limestone filler and metakaolin. *Construction and Building Materials*, *183*, 114-126.
[42] Darweesh, H. H. M. (2020). Influence of sunflower stalk ash (SFSA) on the behavior of Portland cement pastes. *Results in Engineering*, *8*, 100171.
[43] Darweesh, H. H. M. (2021). Utilization of Physalis Pith Ash as a Pozzolanic Material in Portland Cement Pastes. *Journal of Biomaterials*, *5*(1), 1-9.
[44] Panchal, S., Sharma, S., Khan, M. M., Sharma, A., & Roy, A. K. (2017). Effect of glass reinforcement and glass powder on the characteristics of concrete. *International Journal of Civil Engineering and Technology*, *8*(3), 637-647.
[45] ASTM-Standards C170-90 (1993) *Standard Test Method for Compressive Strength of Dimension Stone*, 828-830.
[46] Neville, A. M. (2011) *Properties of Concrete*, 5th ed, UK; Longman Essex.
[47] Hewlett, P. C., & Liska, M. (2017) *Lea's Chemistry of Cement and Concrete*, Butterworth- Heinemann, London.
[48] Darweesh, H. H. M. (2017). Mortar composites based on industrial wastes. *Int. J. Mater. Lifetime*, *3*(1), 1-8.
[49] Voora, V., Larrea, C., & Bermudez, S. (2020). Global Market Report: Bananas
[50] Luxán, M. D., Madruga, F., & Saavedra, J. (1989). Rapid evaluation of pozzolanic activity of natural products by conductivity measurement. *Cement and Concrete Research*, *19*(1), 63-68.
[51] Paya, J., Borrachero, M. V., Monzo, J., Peris-Mora, E., & Amahjour, F. (2001). Enhanced conductivity measurement techniques for evaluation of fly ash pozzolanic activity. *Cement and Concrete Research*, *31*(1), 41-49.
[52] Neville, A. M. (2011) *Properties of Concrete*, 5th Edn, Longman Essex, UK.
[53] Hewlett, P. C. & Liska, M. (2017). *Lea's Chemistry of Cement and Concrete*, Butterworth- Heinemann, London.
[54] Darweesh, H. H. M. (2022) Physico-mechanical properties and microstructure of Portland cement pastes replaced by corn stalk ash (CSA), *International Journal of Chemical Research and Development*, 2(1), 24-33.
[55] Diniz, H. A., dos Anjos, M. A., Rocha, A. K., & Ferreira, R. L. (2022). Effects of the use of agricultural ashes, metakaolin and hydrated-lime on the behavior of self-compacting concretes. *Construction and Building Materials*, *319*, 126087.
[56] Fonseca, T. V., dos Anjos, M. A., Ferreira, R. L., Branco, F. G., & Pereira, L. (2022). Evaluation of self-compacting concretes produced with ternary and quaternary blends of different SCM and hydrated-lime. *Construction and Building Materials*, *320*, 126235.
[57] Faried, A. S., Mostafa, S. A., Tayeh, B. A., & Tawfik, T. A. (2021). The effect of using nano rice husk ash of different burning degrees on ultra-high-performance concrete properties. *Construction and Building Materials*, *290*, 123279.
[58] Tayeh, B. A., Alyousef, R., Alabduljabbar, H., & Alaskar, A. (2021). Recycling of rice husk waste for a sustainable concrete: a critical review. *Journal of Cleaner Production*, *312*, 127734.
[59] Darweesh, H. H. M., & Aboel-Suoud, M. R. (2020). Effect of Agricultural Waste Material on the Properties of Portland Cement Pastes. *Journal of Research & Development in Material Science*, *13*(1), 1360-1367.
[60] Le, H. T., & Ludwig, H. M. (2016). Effect of rice husk ash and other mineral admixtures on properties of self-compacting high performance concrete. *Materials & Design*, *89*, 156-166.
[61] Darweesh, H. H. M., & MR, A. E. S. (2020). Palm ash as a pozzolanic material for portland cement pastes. *To Chemistry Journal*, *4*, 72-85.
[62] Darweesh, H. H. M. (2021). Characterization of coir pith ash blended cement pastes. *Research & Development in Material science*, *RDMS*, *851*(15), 1630-1639.
[63] Sharma, S. K., SandeepPanchal, A. K. R., & Khan, M. M. (2017). Performance comparison of flyash and wollastonite micro-fiber in obtaining self-compacting concrete mixes. *International Journal of Civil Engineering and Technology*, 8(3).
[64] Darweesh, H. H. M. (2022). Effect of banana leaf ash as a sustainable material on the hydration of Portland cement paste. *International Journal of Materials Science*, 4(1): 1-11.